CHAPTER 2
ILMENITE SMELTING PROCESS OVERVIEW

The purpose of this chapter is to introduce the reader to various aspects regarding the ilmenite smelting process. It also combines information from a number of literature resources to provide a consolidated body of data and information on which the work of this study is based.

Although more than one type of furnace design is in industrial use for ilmenite smelting, the current work focuses on a DC furnace like those operated by Namakwa Sands and Ticor South Africa. A schematic of such a furnace is shown in Figure 8.

Because of the secrecy surrounding ilmenite smelting technology (Rosenqvist, 1992) and the resulting lack of published information, the descriptions provided here are for the most part qualitative. Even though this is the case, these descriptions should serve well to introduce a reader that is unfamiliar with the process.

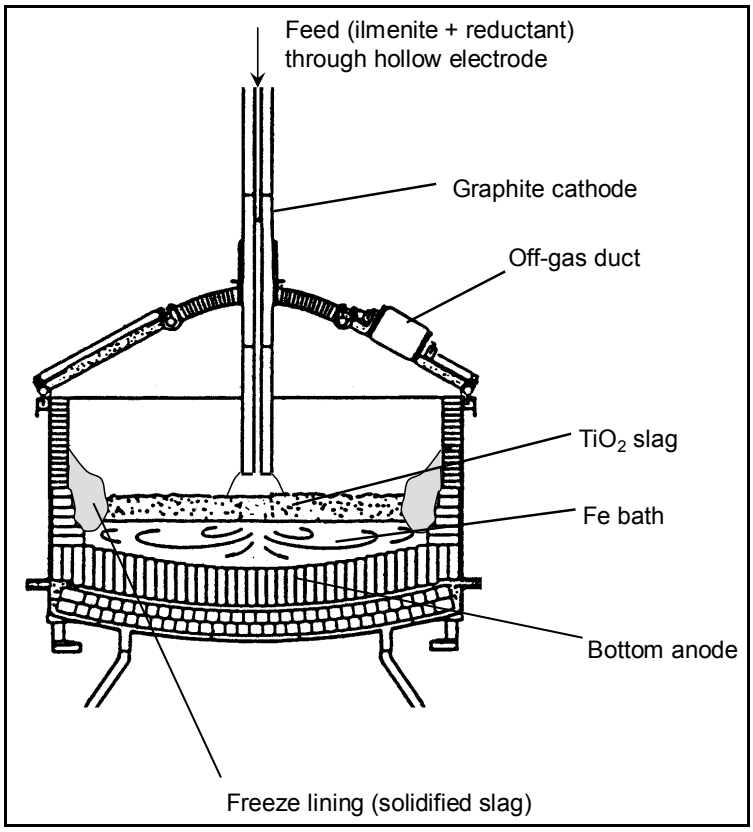

Figure 8 – Schematic representation of an ilmenite-smelting furnace (Pistorius, 1999).

2.1 OPERATIONAL OVERVIEW

The process is operated semi-continuously. Ilmenite, reductant and electrical energy are discharged into the furnace as continuously as possible. The operation is only stopped for adding electrodes, planned and unplanned maintenance, and for process-related incidents like severe slag foaming. Off-gas is extracted from the furnace continuously, while slag and metal are tapped separately in batches.

Ilmenite and reductant enter the furnace through a single hollow graphite electrode that extends down into the furnace through the centre of the furnace roof. Since the electrode is consumed as it delivers energy, it

acts as an additional carbon source. Energy is discharged into the furnace via an open arc between the tip of the electrode and the bath. The only other inputs into the process include air drawn in during periods of negative furnace pressure, and water when leaks are present in the furnace roof, off-gas duct or other water-cooled elements.

Ilmenite is expected to melt quickly as it travels through the arc and into the slag bath. This is due to its relatively low melting point of 1397 °C (FactSage 5.2) and its small particle size of between 100 and 1000 μm. As reductant particles are heated up in the arc and slag bath, these particles devolatilise and possibly break up due to thermal shock. Reduction reactions are expected to take place at the interface between liquid slag and reductant particles. The products of these reactions include gas (primarily CO), slag (enriched in TiO_2 and Ti_2O_3) and iron metal. Some reduction reactions also occur at the interface between the slag and metal bath because of the high carbon content (around 2%) of the metal bath. The products of these reactions are the same as for reduction with reductant particles.

Because of the density difference between metal and slag (metal being denser that slag), metal collects at the bottom of the furnace as a metal bath and slag on top of it as a slag bath. Small metal droplets are present in the slag bath due to the reduction reactions taking place there, but these droplets continuously find their way down to the metal bath or are reabsorbed into the slag. Gas bubbles forming in the slag bath due to reduction reactions rise up through the slag bath and escape into the furnace freeboard.

Metal is extracted from the furnace through a metal tap hole and slag through a slag tap hole. The slag tap hole is situated at a different angular position than the metal tap hole, and higher in the furnace wall than the metal tap hole. This is because the slag bath is floating on top of the metal bath. Off-gas, fumes and dust that continuously rise up into the furnace freeboard are extracted by the off-gas system through a duct installed in the furnace roof.

The off-gas system is operated in such a way that a slight positive pressure is maintained in the furnace freeboard. This is done to prevent air from being drawn into the furnace. Air consumes carbon and oxidises slag, resulting in reduced reductant efficiencies and electrode wear.

2.2 FURNACE CONTROL

The operational personnel and control systems of an ilmenite smelting furnace have the following two primary control objectives:

- Maintain a safe freeze lining thickness to ensure protection of the furnace refractory lining against chemical attack by liquid slag.
- Produce slag with a titanium dioxide content that is within the provided chemical composition specification.

The controlled variables from these objectives are:

- Furnace sidewall temperature

  Sidewall temperature is used as an indirect indication of freeze lining thickness because the state of the freeze lining cannot be measured directly.

- Slag TiO_2 content

  Chemical analyses of tapped slag are used as a measure of this controlled variable.

The manipulated variables used to effect control of the controlled variables are:

- Specific energy input (kWh/ton ilmenite)
- Specific reductant input (ton reductant/ton ilmenite)

Since both manipulated variables have an influence on both controlled variables, the control problem is of the multiple-input-multiple-output (MIMO) type. This together with the dead time associated with measurement of both controlled variables, makes this an interesting control problem that is difficult to solve. It has been reported that the two manipulated variables cannot be changed independently (Pistorius, 1999). This is due to a balance between the enthalpy of the reduction reaction and the enthalpy required to keep the slag at or just above its liquidus temperature. This relationship between the two manipulated variables can be used to simplify the control problem to some degree.

2.3 FURNACE VESSEL

The furnace vessel is shown in Figure 8. It is used to contain the metallurgical process of ilmenite smelting. The vessel is divided into the following four parts for discussion here:

- Hearth
- Sidewalls
- Roof
- Tap holes

2.3.1 Hearth

The hearth of a DC furnace has two roles. The first is to act as the floor of the furnace, containing the metal bath present directly above. The second is to provide the anode connection of the DC electrical circuit.

To contain the hot liquid metal, multiple layers of refractory brick are contained in a steel shell. The bricks are precision manufactured and installed to ensure that no metal will penetrate the lining and burn through after the lining has been heated up and the bricks have completed thermal expansion.

The hearth bricks are usually chosen to have high thermal conductivity, similar to the sidewalls. Air cooling or water cooling is used to extract heat from the outer surface of the hearth and cool it down. Thermocouples are installed in the hearth to generate temperature signals for monitoring the hearth's condition.

The anode connection of the DC electrical circuit can be integrated into the hearth through a number of anode designs. Examples include fins or concentric metal rings built into the anode, metal pins, metal billets and a conductive hearth. The last design is the only one where the contact between the metal bath and the anode is not metal, but rather through electrically conductive refractory brick.

2.3.2 Sidewalls

The sidewalls of an ilmenite-smelting furnace also have a dual purpose. Firstly, similar to the hearth, it must contain the metal and slag baths and the furnace freeboard. Secondly, the sidewalls must extract heat from the slag bath at a high enough rate to establish and maintain a freeze lining of solidified slag on the wall.

The sidewalls are constructed from refractory brick, a steel shell and often a layer of ramming material that is inserted between the bricks and shell to prevent air gaps and ensure good thermal contact. This is especially important on the level of the slag bath where heat extraction is critical.

To further ensure adequate heat extraction on the slag bath level, refractory brick with high conductivity and high density is chosen and water cooling is applied on the outside of the steel shell.

Thermocouples are installed at various vertical, angular and radial positions in the sidewalls. Signals from these instruments are used to monitor the condition of the sidewall refractory lining, and as an indirect measure of freeze lining thickness.

2.3.3 Roof

The roof of the furnace acts as a lid, closing the furnace so that no gas, fumes or dust escapes other than through the off-gas duct. Because the slag bath surface is fluid and at temperatures of between 1650 and 1750 °C, heat is radiated to the furnace roof at high rates. For this reason the roof is water cooled.

One or more inspection ports are usually installed into the roof to enable operational personnel to do visual inspections of the furnace interior.

2.3.4 Tap holes

Tap holes are installed into the furnace sidewalls. One or two metal tap holes are installed on the level of the metal bath, and another one or two slag tap holes are installed at a higher elevation on the level of the slag bath. The tap holes assemblies usually include water cooling aimed at preventing overheating and excessive wear of the refractory lining in the region of the tap holes.

Opening a tap hole is usually done by drilling into the wall up to a specific depth and then using an oxygen lance to burn through to the bath (Noda, 1965). It is closed with a clay plug that is pushed into the hole with a clay gun.

2.4 PROCESS INPUTS

2.4.1 Ilmenite

Ilmenite is the primary input material into the furnace since the purpose of the process is to upgrade ilmenite to a product of higher TiO_2 content. Both DC ilmenite-smelting furnace operations (Namakwa Sands and Ticor South Africa) utilise sand-type ilmenite as feedstock. The particle size of this ilmenite is usually less than 1000 μm.

The major phase in the ilmenite feed is, of course, ilmenite (nominally $FeTiO_3$). Depending on the ore body, some FeO could have been weathered out to leave some rutile (nominally TiO_2) or pseudorutile ($Fe_2Ti_3O_9$)

(Nell, 1999). It is also possible that the ilmenite feed could have been roasted to increase the magnetic susceptibility of ilmenite grains over that of unwanted impurities such as chromium-bearing spinel (nominally $FeCr_2O_4$) and garnet ($(Fe^{2+}, Mg, Mn, Ca)_3(Al, Fe^{3+})_2Si_3O_{12}$) (Nell, 1999). Such roasting is usually oxidising and could result in some of the ferrous iron being converted to ferric iron. The end result is some Fe_2O_3 in an M_2O_3 solid solution with $FeTiO_3$ together with TiO_2 as a separate phase.

Together with the titanium and iron oxides, numerous impurity chemical species also occur. These include CaO, MgO, MnO, ZrO_2, SiO_2, Al_2O_3, Cr_2O_3, P_2O_5, V_2O_5, Nb_2O_5 and possibly others. Some of these species (MgO, MnO) can occur as part of the ilmenite solid solution, while others (SiO_2 and Cr_2O_3) report as separate phases like spinel and garnet as mentioned above. The levels of the various impurities depend on the ore body.

All of the above effects often result in natural ilmenite containing less TiO_2 than the 52.6% by mass of stoichiometric pure ilmenite ($FeTiO_3$).

2.4.2 Reductant

The reductant used in ilmenite smelting is firstly chosen to have low ash content because virtually all of the ash reports in the slag phase as impurities. Secondly, low volatile matter content is preferred. This is to ensure a lower rate of gas evolution from the reductant that can contribute to slag foaming without significantly contributing to reduction. Anthracite and charred coal are therefore mostly used as reductant.

The particle size of the reductant is chosen relatively fine, less than 10 mm. A fine particle size is beneficial for reaction rates in the furnace due to the increased surface area. Too-fine particles are not favoured because these can blow out of the furnace with the off-gas and reduce reductant efficiency.

2.4.3 Graphite Electrodes

The graphite electrodes used in DC ilmenite-smelting furnaces are pre-baked, consisting of more than 99% graphite. The amounts of moisture, ash and volatile matter in these electrodes are negligible. They are manufactured with a hole in the centre through which feed material enters into the furnace.

2.4.4 Refractory Material

Various refractory materials are used in different locations in the furnace lining. All of these will not be discussed here. The material of major importance to this work is the refractory brick used in the sidewalls on the level of the slag bath. These bricks are required to have high thermal conductivity so that heat can be extracted through them to maintain a safe freeze lining thickness. High density, high-MgO material is usually used.

The reason for discussing refractory material under the heading of process inputs is the fact that some of this material is inevitably released into the slag bath through wear of the lining. This is significant because very strict MgO content specifications are usually in place for the slag product destined for pigment production through the chloride process. The reasons behind these strict specifications are explained in paragraph 1.1.7 (page 7).

2.4.5 Water

Leaks in the furnace roof and off-gas duct can result in water entering the furnace. This has a dual effect on the process. Firstly, the water liquid absorbs energy from the process and is converted to water vapour. The energy associated with this effect reduces the energy efficiency of the process. Secondly, the addition of water vapour increases the oxygen partial pressure in the furnace. This adversely affects reductant efficiency. Both these effects are negligible if only small amounts of water are considered, but it could become significant for increased volumes.

Other, more dramatic influences of water include the risk of explosions in the furnace when the conversion from liquid to gas somehow occurs in a confined space; and hydration of the MgO bricks that can severely damage the refractory lining and reduce its life.

2.4.6 Air

During normal operation, air is drawn into the furnace through gaps between furnace roof segments. It is attempted to control the furnace atmosphere at a slight positive pressure, but conditions in the furnace still result in periods of negative pressure.

The oxygen in air can strongly increase the oxygen partial pressure in the furnace. This can be detrimental to reductant efficiency. In terms of energy, the net effect of air entering the furnace should be positive. The heat absorbed by the inert N_2 is less than the heat released by O_2 reacting with CO to form CO_2. This is of course only true if air is not added in excess to what is required for the combustion of CO. This is most likely the case during normal furnace operation.

Large volumes of air are drawn into the furnace when it is placed under negative pressure while an electrode is added or one of the inspection hatches is opened. Under these conditions, air is likely to be present in excess, and it will contribute to cooling the furnace down, consuming some unreacted reductant and possibly oxidising some of the species in the slag.

2.4.7 Energy

Energy can enter the furnace in two ways. Since the furnace is equipped with a DC power supply, discharge of energy through the electric arc is the primary means of energy input. In addition to this, both DC ilmenite-smelting furnace operations (Namakwa Sands and Ticor South Africa) equipped their furnaces with ilmenite pre-heaters. These pre-heaters utilise the chemical energy in the CO rich furnace off-gas to heat ilmenite before discharging it into the furnace.

2.5 PROCESS OUTPUTS

2.5.1 Titania Slag

The furnace is operated with a slag bath temperature of around 1700 °C (Geldenhuis and Pistorius, 1999). Slag is therefore tapped from the furnace around this temperature. The target total TiO_2 content (all Ti reported as TiO_2) of the slag is around 85% (Kahn, 1984).

Refer to paragraph 2.6 for a discussion of the properties of titania slag.

2.5.2 Pig Iron

Heat is extracted at a significant rate from the metal bath through the hearth and sidewalls. For this reason the temperature of the metal bath can be up to 150 °C lower than that of the slag bath (Pistorius, 1999). The carbon content of the metal is around 2% (Pistorius, 1999). It also contains other elements such as Si, Mn, S and P. The levels of such elements in the metal tend to increase as the level of reduction of the slag is increased.

2.5.3 Off-gas

The major species in the off-gas include CO (estimated at between 80 and 90%) as a product from the reduction reactions, and H_2 (estimated at 5 to 15%) from volatiles in the reductant. Some CO_2, H_2O, N_2 and SO_2 are also found. Because of the high CO and H_2 content, this gas is rich in chemical energy. For this reason it is recycled for purposes such as ilmenite pre-heating.

2.5.4 Dust and Fumes

It is likely that thermal shock is experienced by materials as they enter the zone of the electric arc and the bath just beneath it. This can cause reductant and ilmenite particles to break up, producing fine dust particles that are carried into the furnace atmosphere. This is a likely reason for the thick dust cloud present in the furnace freeboard during normal operation. In addition to this, species like Mn and SiO are fumed off at the operating temperatures of the furnace. The dust extracted from the furnace by the off-gas system is enriched in these species.

2.5.5 Energy

Energy leaves the furnace via a number of routes. Liquid slag (at around 1700 °C), liquid metal (at around 1600 °C), and off-gas and dust (at around 1700 °C) carry out large quantities of sensible heat. In addition to this heat is lost through the hearth, sidewalls and roof.

2.6 PROPERTIES OF TITANIA SLAG

Because of the specific importance of titania slag to this project, the relevant properties of this material are discussed below in more detail.

2.6.1 Thermodynamic Data

Valuable work on the thermodynamic properties of the Fe-Ti-O system has been done in recent time. Firstly thermodynamic data from numerous authors were critically assessed and optimised for a number of TiO_2-containing binary systems (Eriksson and Pelton, 1993). The result of this study was, for each binary system, a single set of modified quasichemical model equations describing the Gibbs energy of the liquid slag phase as a function of composition and temperature, and equations for the Gibbs energy of each compound as a function of temperature. The two systems in that work that are of interest to this study are the FeO-TiO_2 and Ti_2O_3-TiO_2 binaries.

The 1993 work was followed up with some experimental work on the stability of pseudobrookite solid solutions in the $FeTi_2O_5$-Ti_3O_5 range, combined with critical assessment of more literature data (Eriksson et al., 1996). All this data was combined and optimised to yield a comprehensive description of the

thermodynamic properties of the $FeTiO_3$–TiO_2–Ti_2O_3–Fe system. This is the system of primary importance to the current study. The data from these studies have been included into the FactSage 5.2 software system (Bale et al., 2002). This software system and the data in its databases were used for much of the work in this study.

In 1999, Pesl and Eriç did measurements in the TiO_2–FeO–Ti_2O_3 ternary system. These measurements have not been incorporated into the FactSage data. For this reason only comparisons between the Pesl and Eriç data and the FactSage calculated values are presented here.

FactSage 5.2 contains three solution phase data sets that can be used for describing the liquid slag phase of interest in this study. These are as follows (FactSage 5.2):

- FACT-SLAGA
  This data set has been approved for the sub-system containing FeO, TiO_2, and Ti_2O_3.
- FACT-SLAGB
  This data set has been approved for the sub-system containing FeO, TiO_2, and Fe_2O_3.
- FACT-SLAG?
  This data set can be used for describing systems containing FeO, TiO_2, Ti_2O_3, and Fe_2O_3. It has however not been thoroughly evaluated and approved by the developers of FactSage.

The FACT-SLAG? data set was the only one available in ChemSage data format for use with the ChemApp library used in this study. Because this data set has not been approved, it was decided to compare it with the FACT-SLAGA data set to determine if significant errors would result from the use of the FACT-SLAG? data. Such comparisons were drawn over a composition range that is applicable to the work of this project, and are shown in Figure 9.

For the most part of the binary diagrams, the difference between results from the two data sets is not visible. It is only on the high TiO_2 side of the diagrams where the FACT-SLAG? results seem to deviate noticeably form the results generated with the approved data set.

The first noticeable difference is on the rutile liquidus line of all three diagrams. The FACT-SLAG? results indicate a slightly lower liquidus temperature on the high TiO_2 end of this line. Such a deviation is not likely to influence the modelling work based on the data set significantly.

The second difference is on the line separating the *pseudobrookite-slag-rutile* region from the *pseudobrookite-rutile* region (the *pseudobrookite-rutile* solidus line). The temperature at which this line ends at the TiO_2 mass fraction upper limit is from 100 to 155 °C lower for the unapproved data set. This inaccuracy causes an overestimation of the amount of liquid slag present in the *pseudobrookite-slag-rutile* region.

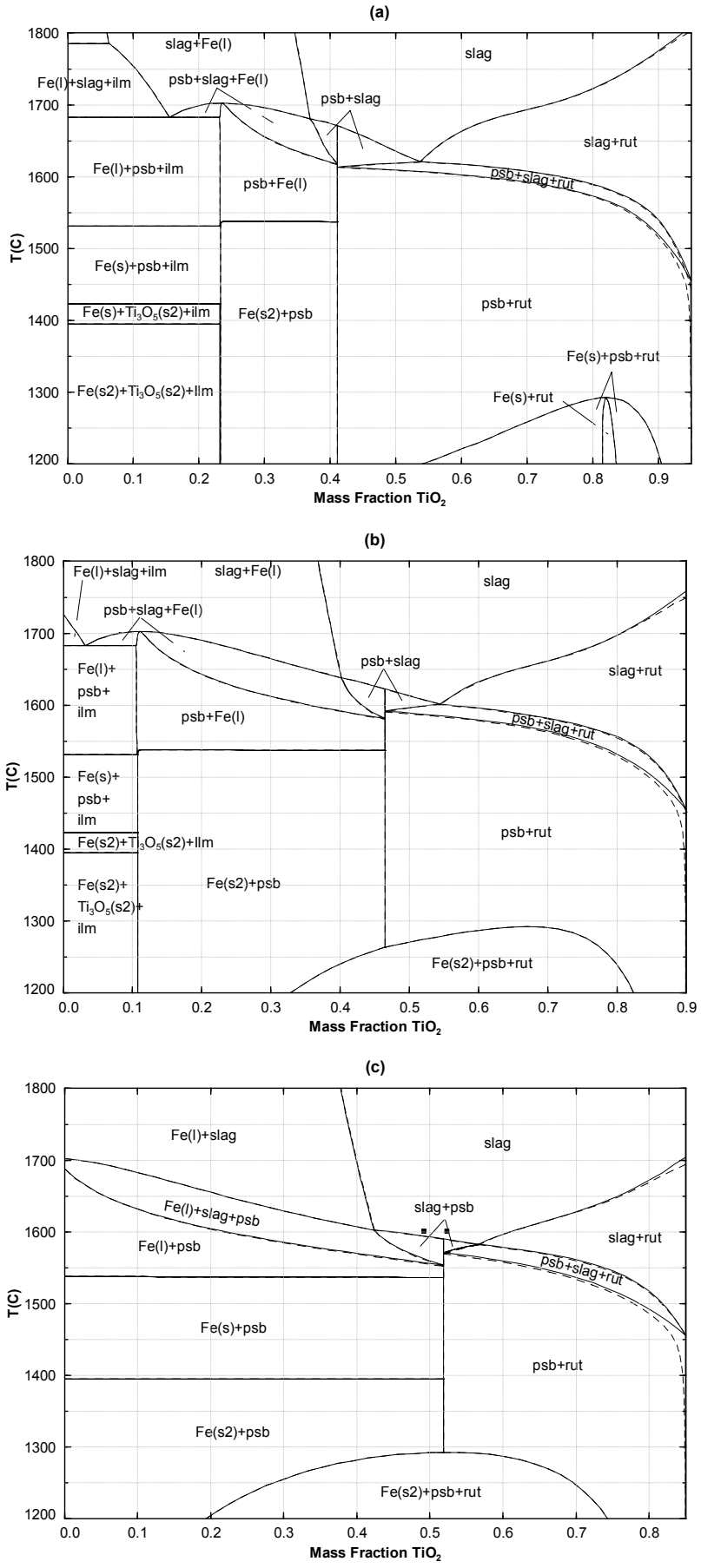

Figure 9 – Constant-FeO binary sections through the TiO_2-FeO-Ti_2O_3 ternary phase diagram.

Solid lines were generated using the FACT-SLAGA data set, and broken lines using the FACT-SLAG? data set in FactSage 5.2.

"rut" = rutile solid solution phase.
"psb" = pseudobrookite solid solution phase.
"ilm" = ilmenite solid solution phase.

Mass percentages of FeO:

(a) %FeO = 5.0
(b) %FeO = 10.0
(c) %FeO = 15.0

Filled squared on (c) indicate data from Pesl and Eriç (1999).

Based on pilot plant slag compositions reported earlier, the TiO_2 (tetravalent titanium, excluding T_2O_3) content of the slag bath is rarely expected to become more than 60% (Pistorius and Coetzee, 2003). This TiO_2 content is therefore chosen as a reference to determine the impact of the inaccuracies on the modelling work that follows. The temperature of the pseudobrookite–rutile solidus line deviates by no more than 2 °C from that of the approved data set. This means that slags with TiO_2 content less than 60% should be adequately described by the FACT–SLAG? data set when modelling reduction reactions, solidification and melting.

In graph (c) of Figure 9 two measured data points from Pesl and Eriç (1999) are shown as filled squared. These two points indicate two differences between the measured data and the data calculated by FactSage 5.2. Firstly, in both cases the measured liquidus temperature is higher than the calculated values. The differences in temperature are around 7 and 13 °C for the two points, which seem insignificant. What is significant, however, is the fact that the measurements indicated that the points lie on different sides of the eutectic groove. The calculated data indicates that the eutectic groove is situated to the right of both measured points.

2.6.2 Liquidus and Solidus Temperatures and Solidification Behaviour

A liquidus diagram was constructed for the TiO_2–$FeTiO_3$–Ti_2O_3 system with the approved data set in FactSage 5.2 and is shown in Figure 10. The dotted lines on this diagram indicate the isothermal boundary between the *slag* region above it, and the *slag–Fe* region below it. This diagram is in good agreement with the conjectural liquidus diagram constructed by Pistorius (1999). Because the conclusion drawn in that work relied strongly on the accuracy of the conjectural liquidus diagram, and because of the good agreement between that diagram and the one in Figure 10, more confidence is placed in the conclusions drawn by Pistorius that energy and reductant inputs into an ilmenite smelter cannot be changed independently.

Figure 10 also shows data as measured by Pesl and Eriç (1999). There are somed significant differences between the measured and calculated data. The measured 1600 °C liquidus curve is mostly situated away from the calculated curve towards the $FeTiO_3$ corner of the diagram. Conversely, the measured 1500 °C liquidus curve is situated away from the calculated curve towards the TiO_2–Ti_2O_3 join. This comparison suggests that for low–FeO compositions, liquidus temperatures are underestimated by the FactSage data, and for higher–FeO compositions, liquidus temperatures are overestimated.

The measured data also places the eutectic groove closer to the M_3O_5 join at both 1500 and 1600 °C. This suggests that the rutile primary phase field can be larger than what the FactSage calculations predict.

Finally, the calculated liquidus lines indicate that the shape of the field where iron metal is stable could be different than what the FactSage calculations predict. The calculations and measurements agree fairly well at 1600 °C, but at 1500 °C the measured data indicates that Fe could be stable at higher TiO_2 content. The boundary of the Fe stability field could therefore have less of a taper towards the $FeTiO_3$ corner of the diagram.

The above differences between measured and calculated data must be taken into account when interpreting the results of this work. All of the calculations done in the present work are based on FactSage 5.2 data.

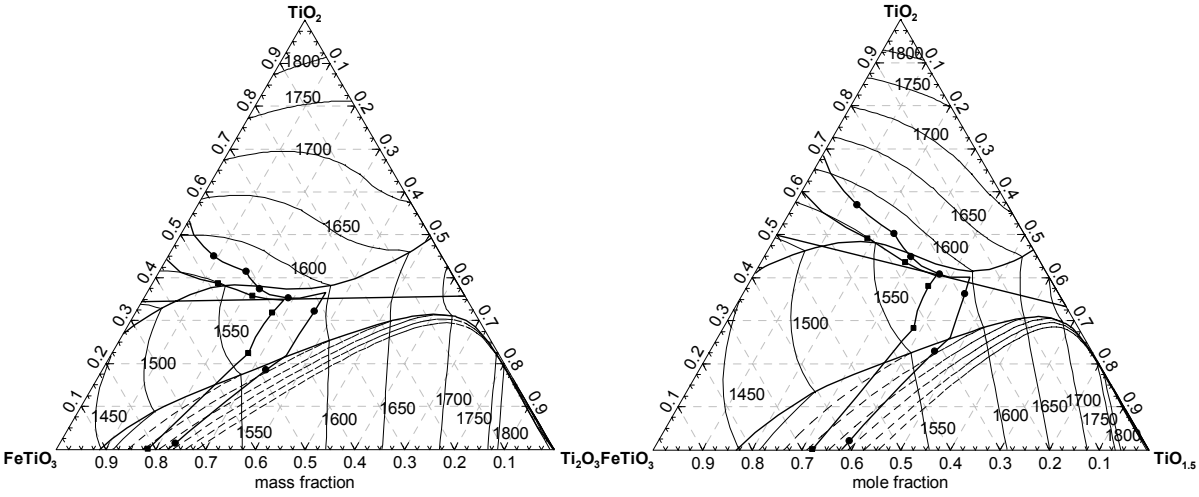

Figure 10 – Liquidus diagram for the TiO_2–$FeTiO_3$–Ti_2O_3 system including Magnéli phases.
Dotted lines indicate the boundary between the *slag* region (above the line) and the *slag–Fe* region (below the line). Thick lines marked with filled squares indicate a measured 1500 °C liquidus line (Pesl and Eriç, 1999). Thick lines marked with filled circles indicate a measured 1600 °C liquidus line (Pesl and Eriç, 1999). The top curved thick line indicates the eutectic groove composition. The bottom curved thick line indicates the non-isothermal boundary between the slag region and the slag–Fe region. The straight thick line indicates the M_3O_5 join.

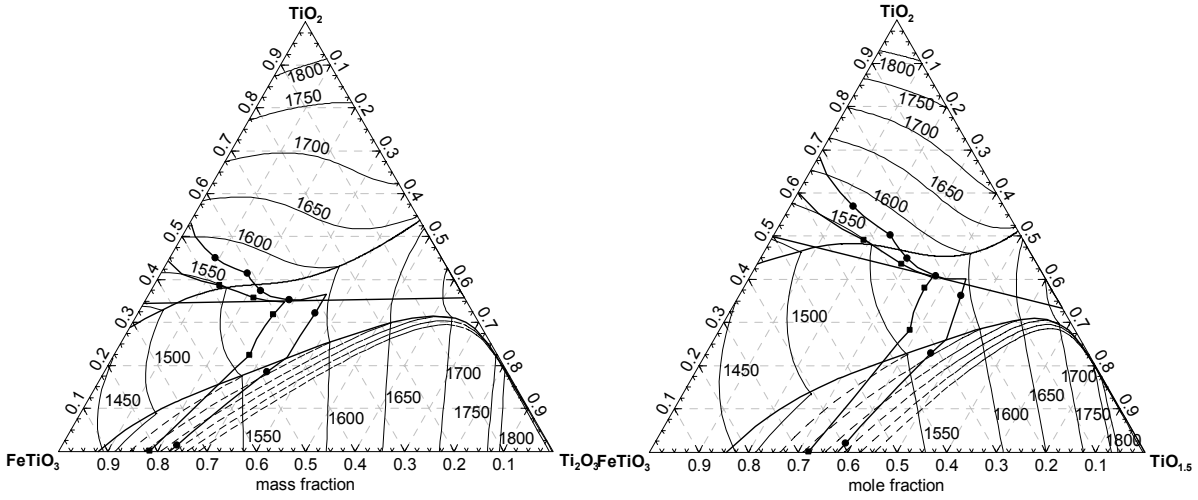

Figure 11 – Liquidus diagram for the TiO_2–$FeTiO_3$–Ti_2O_3 system excluding Magnéli phases
Dotted lines indicate the boundary between the *slag* region (above the line) and the *slag–Fe* region (below the line). Thick lines marked with filled squares indicate a measured 1500 °C liquidus line (Pesl and Eriç, 1999). Thick lines marked with filled circles indicate a measured 1600 °C liquidus line (Pesl and Eriç, 1999). The top curved thick line indicates the eutectic groove composition. The bottom curved thick line indicates the non-isothermal boundary between the slag region and the slag–Fe region. The straight thick line indicates the M_3O_5 join.

Figure 11 shows a liquidus diagram for the same system with Magnéli phases omitted. The reason for doing this is that these phases are not detected in high-titania slags. The liquidus diagrams in Figure 11 were therefore used during this study.

The data measured by Pesl and Eriç (1999) is also shown on Figure 11. Agreement between measurements and calculated values are worse on this diagram than on Figure 10 if one considers the relative positions of the eutectic grooves. This is to be expected if one consider that Pesl and Eriç (1999) did take Magnéli phases into account.

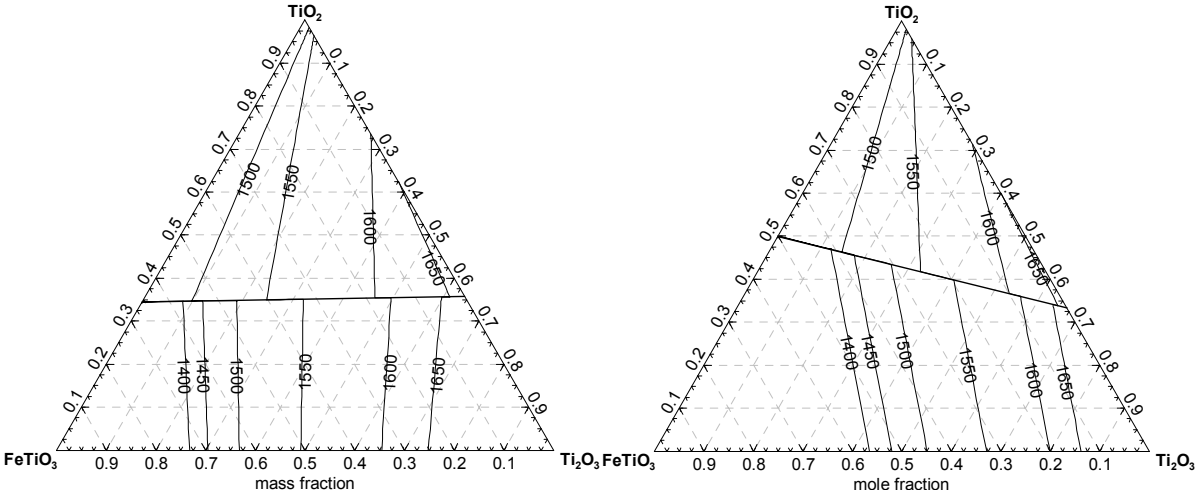

Figure 12 – Solidus diagram for the TiO_2–$FeTiO_3$–Ti_2O_3 system including Magnéli phases.
The straight thick line indicates the M_3O_5 join. Only slag is considered in this diagram. The solidus lines indicate the boundaries of regions, to the right of the lines, in which only solid slag occurs.

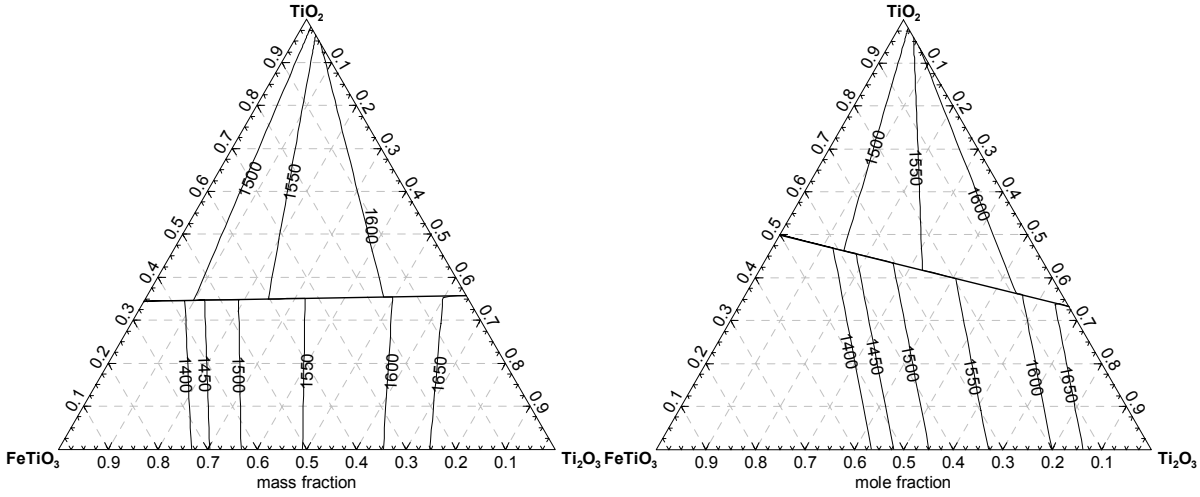

Figure 13 – Solidus diagram for the TiO_2–$FeTiO_3$–Ti_2O_3 system excluding Magnéli phases
The straight thick line indicates the M_3O_5 join. Only slag is considered in this diagram. The solidus lines indicate the boundaries of regions, to the right of the lines, in which only solid slag occurs.

Figure 12 and Figure 13 shows solidus diagrams of the TiO_2–$FeTiO_3$–Ti_2O_3 system. Again the first set includes Magnéli phases and the second does not.

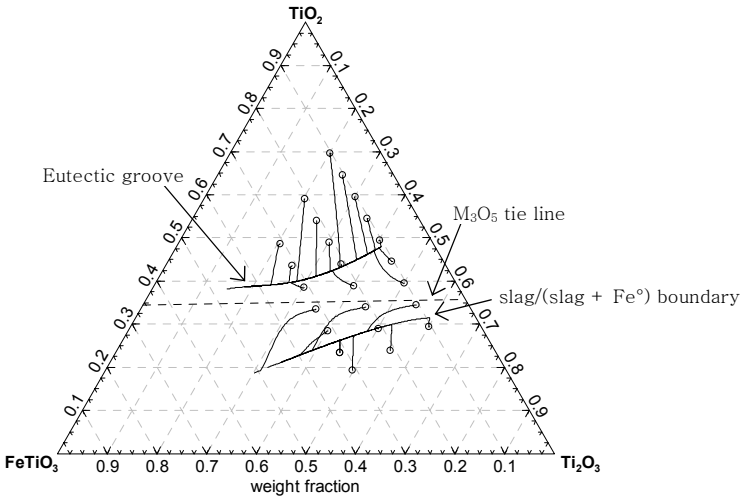

Figure 14 – Liquid slag composition trajectories during solidification.
The dotted line indicates the Ti_3O_5–$FeTi_2O_5$ join. Initial composition indicated by circles and trajectories by solid lines.

Another useful view on the behaviour of the system under consideration, given the importance of solidification and melting behaviour in this study, is the composition trajectory of the liquid slag phase during solidification. Figure 14 shows a grid of initial liquid slag compositions above the liquidus temperature (circles) and associated composition trajectories (solid lines) of the liquid slag phase as the system is cooled down to its solidus temperature. This diagram gives an indication of the direction in which solidification and melting phase equilibria can influence the composition of the slag bath. Figure 14 is based on the FACT–SLAG? data set and therefore contains some inaccuracies.

It is evident from Figure 14 that the composition of liquid slag with a starting composition above the M_3O_5 join is modified through solidification to eventually end up in the eutectic groove visible in Figure 9. Liquid slag with starting composition below the Ti_3O_5–$FeTi_2O_5$ join tends to drift toward the boundary of the phase field where iron metal becomes stable. The cases converging in the eutectic groove is a demonstration of the phase chemistry behaviour during solidification that was proposed as the origin of the compositional invariance of ilmenite smelter slag close to the M_3O_5 composition (Pistorius, 2002).

2.6.3 Heat Capacity

Figure 15 shows temperature vs. enthalpy curves for three different slag compositions under equilibrium conditions, as calculated with FactSage 5.2. For these three compositions, the latent heat of fusion represents approximately 27% of the enthalpy required to heat the material from 0 °C up to its liquidus temperature. This is a significant point, since the latent heat of fusion acts as 'buffer' between events occurring inside the furnace, and the brick portion of the furnace wall in which thermocouples are installed. Even without this buffer a temperature change taking place at the hot face of the freeze lining will take a long time to be detected by a thermocouple installed in the brick. The latent heat of fusion adds to this time lag, and ultimately to the degree of difficulty of the freeze lining control problem.

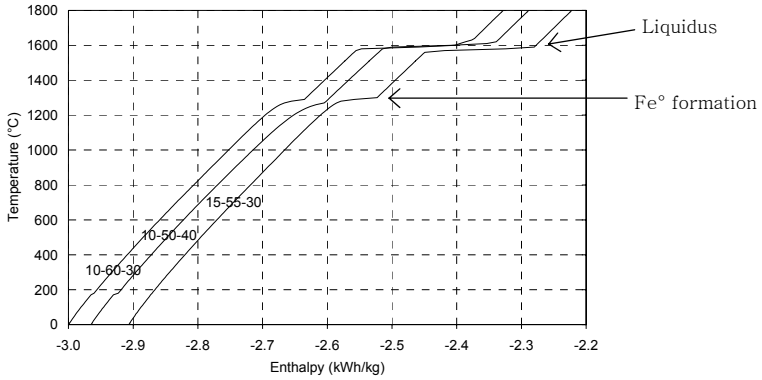

Figure 15 – Temperature vs. enthalpy curves for three difference slag compositions.
Composition indicated as $FeO-TiO_2-Ti_2O_3$ mass percentages.

Two distinctive changes in slope are visible on Figure 15. The first is at around 1600 °C where the slag converts from solid to liquid or vice versa depending on whether temperature is increasing or decreasing. The second is visible just below 1300 °C. Below this temperature iron metal becomes stable. This can be verified on Figure 9 (page 21).

2.6.4 Viscosity

The viscosity of high-titania slag has been determined previously (Handfeld and Charette, 1971). The values reported by them are around 0.03 kg/ms for slags above their liquidus temperature. This is several orders of magnitude less than the viscosity (10^6 kg/ms) of SiO_2 at its melting point (1727 °C) (Pistorius and Coetzee, 2003).

This viscosity data is of relevance to this work since it determines the validity of assumptions made about the slag being ideally mixed. Due to the strong stirring that is known to occur in the slag bath, and the low viscosity of the slag, assuming ideal mixing in the slag bath seems to be valid.

2.6.5 Thermal Conductivity

Due to the nature of this study, the thermal conductivity of solid high-titania slag is of great importance. Little published data is available on this. The value of 1.0 W/(m.K) that was used in this text was obtained from Pistorius (2004, 2004b).

2.6.6 Compositional Invariance

Pistorius (1999) identified a relationship between the Ti_2O_3 and FeO content of high-titania slag. Work has been done to determine the phenomena that cause this relationship (Pistorius 2002; Pistorius and Coetzee 2003; Pistorius 2003; Pistorius 2004). Further study to determine the cause of this compositional invariance was part of the scope of this study. CHAPTER 10 is therefore dedicated to this subject.